Effect of Measurement Geometry on Weak Localization in Short Wires

V. Chandrasekhar and D. E. Prober
Section of Applied Physics, Yale University, P.O. Box 2157, New Haven, Connecticut 06520

P. Santhanam
IBM Research Division, T. J. Watson Research Center, Yorktown Heights, New York 10598
(Received 1 August 1988)

The effect of measurement-probe geometry on the weak-localization magnetoresistance of short silver wires is investigated. The wires have lengths comparable to the electron phase coherence length l_ϕ, which is a few microns at 1 K. The influence of different probe geometries is seen directly in the magnitude and shape of the low-field magnetoresistance of these wires. We have extended the theory of weak localization to include the effects of the measurement geometry, and find good quantitative agreement with experiment.

PACS numbers: 71.55.Jv, 72.15.Gd, 72.15.Lh

Studies of electrical transport in small (mesoscopic) systems have dramatically increased our understanding of electron quantum interference effects, including electron localization[1] and conductance fluctuations.[2] When the system size L is less than or comparable to the electron phase-breaking length l_ϕ, the measuring probes directly influence these interference effects. Recent experimental[3] and theoretical[4] studies on this subject have focused on conductance fluctuations. However, weak localization (WL) can provide significant new physical insight into the effects of measurement-probe geometry. First, in the theory of WL, it is much simpler to treat complex measurement geometries. Theoretical work on conductance fluctuations has been restricted to quasi-one-dimensional geometries. Second, the influence of different geometries can be seen *directly* in the low-field magnetoresistance (MR), without recourse to detailed statistical analysis. The first experiments on WL in short wires were by Masden and Giordano,[5] but because of a lack of MR data and complications from electron-electron interactions, their results were not conclusive.

In this Letter, we report on detailed measurements of the WL magnetoresistance of short, narrow Ag wires in two different probe configurations, shown in Fig. 1. Figure 1(a) shows a short wire with four *narrow* measurement probes. Figure 1(b) shows a short wire with *wide* probes: two two-dimensional (2D) probes and two one-dimensional (1D) probes. We are able to see the influence of the different probe configurations in the magnitude and the shape of the low-field MR of these wires. We have extended the theory to account for 2D probes, and find good quantitative agreement with experiment.

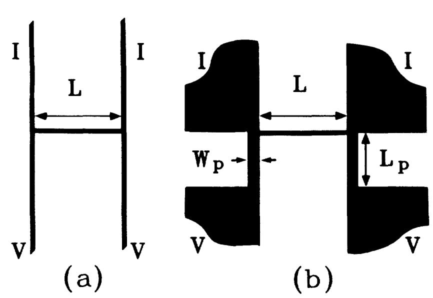

FIG. 1. Schematic of probe geometry of short wires: (a) Short wire, length L, with narrow probes. (b) Short wire with wide probes; $L_P \sim 3$ μm, $W_P \sim 0.3$ μm.

The wires in this study were prepared by thermal evaporation onto oxidized silicon substrates previously patterned with use of a bilayer electron-beam technique.[6] They had widths $W \sim 40$ nm, thickness 20 nm, and sheet resistances $R_\square \sim 1.0$–2.5 Ω. Sample dimensions were measured in a scanning electron microscope. Long wires, with length $L \sim 53$ μm, and wide 2D films were codeposited for comparison of material properties. The relevant properties of the wires are summarized in Table I. The MR was measured in a perpendicular field with use of a four-terminal ac bridge in the temperature range 1.25–20 K. Figure 2(a) shows the MR, $\delta R/R = [R(H) - R(0)]/R$, of the $L \sim 1.3$-μm wires and their codeposit-

TABLE I. Sample parameters. $R_\square$ is at 4.5 K. Narrow-probe configuration corresponds to Fig. 1(a), wide-probe configuration to Fig. 1(b). Values of l_ϕ are at 1.25 K, except for sample B, for which a satisfactory fit at 1.25 K was not possible because of the presence of conductance fluctuations. $l_{s.o.}$ for a particular sample was found to be independent of temperature (Ref. 7). Samples A, B, C, and E were codeposited; samples D and F were codeposited.

Sample	$R_\square$ (Ω)	L (μm)	Probe config.	l_ϕ (1.25 K) (μm)	$l_{s.o.}$ (μm)
A	1.4	1.3	Narrow	2.2	0.43
B	1.4	1.4	Wide	1.3 (3.5 K)	0.41
C	2.2	4.9	Narrow	1.5	0.30
D	1.1	4.8	Wide	3.0	0.65
E	1.4	53	(Long wire)	2.3	0.39
F	1.2	53	(Long wire)	2.9	0.51

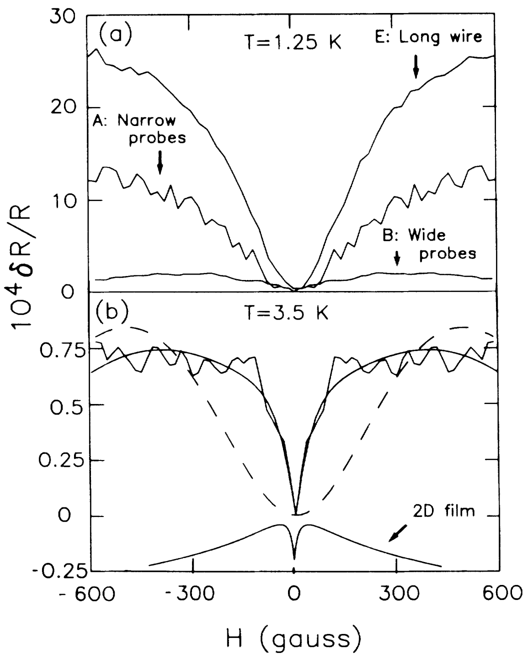

FIG. 2. (a) Magnetoresistance at 1.25 K, samples A, B, and E. For samples A and B, only the symmetry component is shown. (b) Symmetric component of the magnetoresistance of sample B at 3.5 K. Solid line, fitted with full theory, Eq. (4), with $l_\phi = 1.3$ μm, $l_{s.o.} = 0.43$ μm. Dashed line, best fit with Eq. (3), $l_\phi = 0.62$ μm, $l_{s.o.} = 0.46$ μm. Bottom curve, theoretical weak-localization magnetoresistance of a 2D film with the same $R_\square$. The zero of this curve is offset for clarity.

ed long wire. The most striking difference between the three samples is in the magnitude of the MR. The MR of the short wire with narrow probes is about half that of the long wire, and the MR of the short wire with wide probes is less than a tenth of that of the long wire.

In order to explain these results quantitatively, we must incorporate the effects of the measurement probes in the theory of WL. Theoretically, WL is described by the particle-particle propagator, $C(\mathbf{r},\mathbf{r}')$, which is a solution of the diffusion equation. In the absence of magnetic field and spin-dependent scattering,[8]

$$(-\nabla^2 + l_\phi^{-2}) C(\mathbf{r},\mathbf{r}') = \delta(\mathbf{r},\mathbf{r}')/\hbar D\,, \tag{1}$$

where $D = \frac{1}{3} v_F l$ is the diffusion constant, v_F is the Fermi velocity, and l ($\ll l_\phi$) is the elastic mean free path. The fractional change in resistance due to WL is given by $\Delta R/R = (2e^2 D/\pi\sigma) C_0$ where σ is the conductivity and C_0 is $C(\mathbf{r},\mathbf{r})$ averaged over the sample.[8,9] The influence of the probes is taken into account by the application of the appropriate boundary conditions to Eq. (1). Doucot and Rammal[9] have developed a formalism for solving Eq. (1) for a network of wires of equal width W, with the boundary condition that $C(\mathbf{r},\mathbf{r}')$ be continuous at each wire intersection. This formalism is equivalent to the assumption that the phase coherence decays at a length scale l_ϕ into the probes.[10] For the narrow-probe geometry of Fig. 1(a), when the length of each measurement probe $L_p \gg l_\phi$, one obtains[10]

$$\frac{\Delta R}{R} = \frac{R_\square}{\pi\hbar/e^2} \frac{l_\phi}{W} \frac{5\coth(L/l_\phi) - 3(l_\phi/L) + 4}{5 + 4\coth(L/l_\phi)}\,. \tag{2}$$

In the limit of $L \gg l_\phi$, this reduces to the usual long-wire result[8]

$$\frac{\Delta R}{R} = \frac{R_\square}{\pi\hbar/e^2} \frac{l_\phi}{W}\,. \tag{3}$$

In the opposite limit of $L \ll l_\phi$, Eq. (2) reduces to *half* the result of Eq. (3). $C(\mathbf{r},\mathbf{r}')$ measures the enhanced probability that a diffusing electron will return to the point $\mathbf{r}$ because of quantum interference. An electron which diffuses into a probe which is within a distance l_ϕ of $\mathbf{r}$ has a reduced chance of returning to $\mathbf{r}$; the greater the number of such probes, the lower the probability $C(\mathbf{r},\mathbf{r})$. The majority of points in the long wire are more than l_ϕ away from the probes, and therefore have, in essence, only *two* wires into which diffusion can occur. In contrast, each point in the short wire with narrow probes can diffuse into *four* measurement probes, leading to a factor of 2 *reduction* in the MR.

We shall now extend the approach of Doucot and Rammal to solve Eq. (1) in the geometry of Fig. 1(b), the short wire with *wide* probes. We present here an outline of the calculation; the details will be given elsewhere. First we solve Eq. (1) in the 1D wire, 2D probes, and 1D probes, and demand that $C(\mathbf{r},\mathbf{r}')$ be continuous at the ends of the wire. Assuming that the length of the voltage probes $L_p \gg l_\phi$, we obtain

$$\frac{\Delta R}{R} = \frac{R_\square}{\pi\hbar/e^2} \frac{l_\phi}{W} \frac{(\beta^2+\alpha^2)\coth(L/l_\phi) - (l_\phi/L)(\beta^2-\alpha^2) + 2\alpha\beta}{\beta^2+\alpha^2+2\alpha\beta\coth(L/l_\phi)}\,, \tag{4}$$

where $\alpha = W/l_\phi$, $\beta = \beta_1 + \beta_2$, $\beta_1 = W_p/l_{\phi p}$, $\beta_2 = (\pi/2) \times \ln(2l_{\phi 2D}/l)$, W_p is the width of the probes, $l_{\phi p}$ is the phase-breaking length in the probes, and $l_{\phi 2D}$ is the phase-breaking length in the pads; the last two can be different from l_ϕ in the wire.[7] β_1 contains the effects of the 1D probes and β_2 the effects of the 2D probes.[11] It is useful to look at the limits of Eq. (4). As expected, in the limit of $L \gg l_\phi$, we regain the long-wire result, Eq. (3). In the opposite limit of $L \ll l_\phi$, $\Delta R/R \propto \ln(2l_{\phi 2D}/l)$, characteristic of 2D localization.[1] As before, the amplitude of $C(\mathbf{r},\mathbf{r}')$ is determined by the diffusion into the probes. Since the probability of diffusion into 2D probes is greater than that into narrow 1D probes, the amplitude of the MR is reduced compared to the short wire with narrow probes. The 2D nature of the probes also shows up explicitly in the shape of the MR. This shape is qualitatively different from the one obtained by assuming that $C(\mathbf{r},\mathbf{r}')=0$ in the probes.[10]

The formulation of including spin-orbit scattering[12] and the effect of an external magnetic field H on 1D wires is described in detail in Ref. 7. For the wide probes,[13] Fig. 1(b), a magnetic field modifies the value of β_2 to

$$\beta_2=\pi/[\ln(4H_0/H)-\psi(\tfrac{1}{2}+H_\phi/H)],$$

where ψ is the digamma function, $H_0=\hbar c/4el^2$, and $H_\phi=\hbar c/4el_{\phi 2D}^2$. The weak-localization MR is symmetric in the field. The experimental MR also contains contributions from symmetric and antisymmetric conductance fluctuations.[14] We therefore fit only the envelope of the symmetric component of the experimental MR.

We first discuss the qualitative features of the MR of the short wires. Figure 2(b) shows the MR of the short wire with *wide* probes, sample B, at 3.5 K, where $L\sim l_\phi$. The MR shows a sharp rise near zero field. This sharp rise is similar to the weak-localization MR of a 2D film, also shown in Fig. 2(b), suggesting that it may be due to the influence of the 2D probes. A fit to Eq. (4), which incorporates the effect of the 2D probes, shows that this is indeed the case. The dashed line shows the best least-squares fit to the long-wire formula, Eq. (3), with two adjustable parameters, l_ϕ and the spin-orbit length $l_{\mathrm{s.o.}}$. This fit, as expected, is unable to account for the sharp rise. Similar unsatisfactory fits are found at other temperatures and in other wires with wide probes when $L\leq 1.5l_\phi$. The sharp rise in the MR is not seen in the short wires with narrow probes, samples A and C. Data for these wires are fitted well with the appropriate formula, Eq. (2).

An important self-consistency check on the theory is to compare the values of l_ϕ inferred from the theory fits to those obtained for the codeposited long wires. By fitting the MR of the short wires at all temperatures, we determined l_ϕ vs L/l_ϕ^{LW}, where l_ϕ^{LW} is l_ϕ for the respective long wire. This is plotted in Fig. 3 on a log-log scale. The solid lines (with slopes -1) are, by definition, l_ϕ for codeposited long wires. Data for the two short wires with *wide* probes are shown in Fig. 3(a). The solid circles shows the values of l_ϕ inferred from the appropriate formula, Eq. (4). Figure 3(a) shows that these values of l_ϕ are consistent with those obtained for the codeposited long wire.[15] For comparison, we show the values of l_ϕ inferred from fits with the long-wire formula, Eq. (3), for the $\sim$5-μm wire, sample D. For this sample, fits with Eq. (3) are reasonable, but the values of l_ϕ inferred are too small by a factor of ~ 1.8 at the lowest temperature, where $L\sim 2l_\phi$. The shape of the MR of sample B at $L\leq 1.5l_\phi$ precludes fits with the long-wire formula.

The values of l_ϕ for the two short wires with *narrow* probes inferred from Eq. (2) are shown in Fig. 3(b),

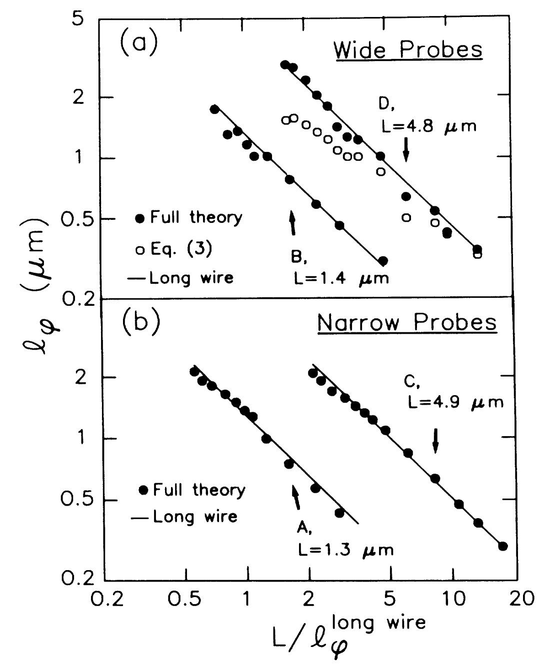

FIG. 3. l_ϕ vs L/l_ϕ^{LW}, for $T=1.25$–20 K. Solid lines, with slopes -1, are data for long wires, samples E and F. (a) Data for short wires with wide probes, samples B and D. Solid circles from fits with full theory, Eq. (4); open circles from fits to the long-wire formula, Eq. (3). (b) Data for short wires with narrow probes, samples A and C. Solid circles from fits with Eq. (2). Data for sample C have been normalized to the $R_\square$ and W of sample E.

along with l_ϕ for the codeposited long wire, sample E. (The values of l_ϕ for sample C have been adjusted to take into account the dependence of l_ϕ on $R_\square$ and W.[7,8]) Here again we find that the values of l_ϕ inferred for the short wires are in good agreement with those found in the long wire.

In addition to weak localization, we have also studied the amplitude of the conductance fluctuations in the two different probe configurations. The conductance fluctuations were measured at higher magnetic fields in the temperature range 1.25–4.6 K. Comparing the two $L\sim 1.3$-μm wires (samples A and B), we find that the rms value of the conductance fluctuations, ΔG, for the sample with wide probes is typically half that for the sample with narrow probes. For example, at 1.25 K, $\Delta G=0.11e^2/h$ for sample B; $\Delta G=0.21e^2/h$ for sample A. This reduction in amplitude for sample B is similar to the reduction in the amplitude of the weak-localization MR. We again attribute this to the presence of the wide probes.

In conclusion, we find that WL provides a simple and physically insightful means of investigating the effect of measurement-probe geometry on quantum interference. We believe that the approach we have developed can be used to extend the theory for other quantum interference effects to more complex geometries.

We thank T. E. Kopley for providing the oxidized silicon substrates for the experiments, Dr. Alan Pooley for the scanning electron micrographs, and A. D. Stone, R. A. Webb, and R. G. Wheeler for useful comments. This work was supported by NSF Grant No. DMR-8505539 and conducted in the Yale University Center for Microelectronic Materials and Structures.

---

[1]P. A. Lee and T. V. Ramakrishnan, Rev. Mod. Phys. **57**, 287 (1985); G. Bergmann, Phys. Rep. **107**, 1 (1984)

[2]P. A. Lee, A. D. Stone, and H. Fukuyama, Phys. Rev. B **35**, 1039 (1987); S. Washburn and R. A. Webb, Adv. Phys. **35**, 375 (1986).

[3]A. Benoit, C. P. Umbach, R. B. Laibowitz, and R. A. Webb, Phys. Rev. Lett. **58**, 2343 (1987); W. J. Skocpol, P. M. Mankiewich, R. E. Howard, L. D. Jackel, and D. M. Tennant, Phys. Rev. Lett. **58**, 2347 (1987); C. P. Umbach, P. Santhanam, C. van Haesondonck, and R. A. Webb, Appl. Phys. Lett. **50**, 1289 (1987).

[4]S. Maekawa, Y. Isawa, and H. Ebisawa, J. Phys. Soc. Jpn. **56**, 25 (1987), and **55**, 2523 (1986); M. Buttiker, Phys. Rev. B **35**, 4123 (1987); R. A. Serota, S. Feng, C. Kane, and P. A. Lee, Phys. Rev. B **35**, 5031 (1987); H. U. Baranger, A. D. Stone, and D. P. DiVincenzo, Phys. Rev. B **37**, 6521 (1988); S. Hershfield and V. Ambegaokar, Phys. Rev. B **38**, 7909 (1988).

[5]J. T. Masden and N. Giordano, Phys. Rev. Lett. **49**, 819 (1982). See also K. K. Choi, D. C. Tsui, and S. C. Palmateer, Phys. Rev. B **33**, 8216 (1986). The low $R_\square$ of our films and the absence of significant magnetic scattering gives large values of l_ϕ. In this regime, weak-localization effects are suppressed by small magnetic fields, whereas electron-electron interaction effects are not. This enables us to distinguish between the weak localization and electron-electron contributions.

[6]M. J. Rooks, S. Wind, P. McEuen, and D. E. Prober, J. Vac. Sci. Technol. B **5**, 318 (1987).

[7]See, for example, P. Santhanam, S. Wind, and D. E. Prober, Phys. Rev. B **35**, 3188 (1987), and references therein.

[8]B. L. Alt'shuler, A. G. Aronov, D. E. Khmelnitskii, and A. I. Larkin, in *Quantum Theory of Solids,* edited by I. M. Lifshitz (Mir, Moscow, 1982), and references therein; B. L. Alt'shuler, A. G. Aronov, and A.Yu. Zyuzin, Zh. Eksp. Teor. Fiz. **86**, 709 (1984) [Sov. Phys. JETP **59**, 415 (1984)]. Note that the magnetoresistance due to weak localization is defined as $\delta R = \Delta R(H) - \Delta R(0)$.

[9]B. Doucot and R. Rammal, Phys. Rev. Lett. **55**, 1148 (1985), and J. Phys. (Paris) **47**, 973 (1986).

[10]P. Santhanam, Phys. Rev. B **35**, 8737 (1987).

[11]It is interesting to note that by taking $\beta_2 = 0$ (no 2D probes) and $\beta_1 = 2\alpha$ (two 1D probes on either end of the wire) in Eq. (4), one regains Eq. (2). The β term in Eq. (4) is the one that contains information about the probes. For more complicated probe configurations, Eq. (4) remains the same, but the form of β is modified.

[12]No saturation of the MR in the long wires was seen as the temperature was reduced, so we conclude that paramagnetic impurity scattering is insignificant.

[13]$l_{\phi 2D}$ was determined by analyzing the weak-localization magnetoresistance of the codeposited 2D film.

[14]M. Buttiker, Phys. Rev. Lett. **57**, 1761 (1986); A. D. Benoit, S. Washburn, C. P. Umbach, R. B. Laibowitz, and R. A. Webb, Phys. Rev. Lett. **57**, 1765 (1986).

[15]For $L \ll l_\phi$, one might not expect l_ϕ and l_ϕ^{LW} to be identical. However, the consistency in the values of l_ϕ we obtain for samples with different probe geometries shows that this is not the case for $L \sim l_\phi$.